Available online at www.sciencedirect.com
SCIENCE DIRECT
Biochemical and Biophysical Research Communications 346 (2006) 108–115
BBRC
www.elsevier.com/locate/ybbrc

Interaction between the cellular prion (PrP^C) and the 2P domain K^+ channel TREK-1 protein

Alberto Azzalin [a], Valentina Ferrara [a], Agustina Arias [a], Silvia Cerri [b], Debora Avella [b], Maria Bonaria Pisu [b], Rosanna Nano [b], Graziella Bernocchi [b], Luca Ferretti [a], Sergio Comincini [a,*]

[a] *Dipartimento di Genetica e Microbiologia, Università di Pavia, Pavia, Italy*
[b] *Dipartimento di Biologia Animale, Università di Pavia, Pavia, Italy*

Received 28 April 2006
Available online 24 May 2006

Abstract

The cellular prion protein (PrP^C) is a highly conserved protein throughout the evolution of mammals and therefore is thought to play important cellular functions. Despite decades of intensive researches, the physiological function of PrP^C remains enigmatic. Differently, in particular pathological contexts, generally referred as transmissible spongiform encephalopathies, a conformational isoform of PrP^C, i.e., PrP^{Sc}, is considered the causative agent of these diseases. In this study, we investigated putative PrP^C cellular functions through the identification of PrP^C protein interactants. Using a bacterial two-hybrid approach, we identified a novel interaction between PrP^C and a two-pore potassium channel protein, TREK-1. This interaction was further verified in transfected eukaryotic cells using co-immunoprecipitation and confocal microscopic analysis of the fluorescent transfected proteins. Importantly, in the cerebellar cortex, the endogenous PrP^C and TREK-1 proteins exhibited co-localization signals in correspondence of the Purkinje cells. Furthermore, a deletion mapping study defined the carboxyl-terminal regions of the two proteins as the possible determinants of the PrP^C–TREK-1 interaction. Our results indicated a novel PrP^C interacting protein and suggested that this complex might be relevant in modulating a variety of electrophysiological-dependent cellular responses.

Keywords: Prion protein; TREK-1; Protein interaction

The cellular prion protein (PrP^C) is a glycosylphosphatidylinositol (GPI)-anchored protein that is expressed in many tissues, with the highest level in peripheral (PNS) and central nervous system (CNS) [1]. PrP^C is a molecule of approximately 250 amino acids in length and contains an amino-terminal signal peptide for endoplasmic reticulum targeting and a carboxyl-terminal peptide for membrane GPI-anchoring. During its biosynthesis, PrP^C undergoes post-translational modifications such as the addition of amino-linked oligosaccharide chains and the formation of a disulfide bond [2]. PrP^C is predominantly located on the cell surface, in specific lipid membrane domains called "rafts" [3]; indeed, other data suggested that PrP^C is also present in endocytic transport vesicles and exhibits a complex sub-cellular trafficking [4]. Besides, different PrP^C membrane conformations were hypothesized, and it was suggested that these alternative topologies might play a role in the pathogenesis of the prion diseases (reviewed in [5]).

PrP^C has a fundamental role in the aetiology of a group of fatal neurodegenerative diseases known as transmissible spongiform encephalopathies (TSE). These pathologies include Creutzfeldt-Jakob disease (CJD) in human, bovine spongiform encephalopathy (BSE) in cattle, scrapie in sheep and goats, and chronic wasting disease (CWD) in deer and elk [6]. Prion diseases are characterized by the abnormal accumulation of a prion pathological isoform,

* Corresponding author. Fax: +39 382 528496.
E-mail address: sergio.c@ipvgen.unipv.it (S. Comincini).

0006-291X/$ - see front matter © 2006 Elsevier Inc. All rights reserved.
doi:10.1016/j.bbrc.2006.05.097

generally referred to as PrP^{Sc} [7]. Additionally, these diseases exhibit various neurological symptoms and common histopathological features such as the spongiform degeneration of the CNS, reactive gliosis, neuronal loss, and formation of amyloid plaques [8].

To investigate into the function of PrP^{C}, several lines of prion knock-out mice were produced. These mice were generally healthy except for weak alterations such as variations in circadian rhythms or increased locomotor activities; moreover, development of scrapie symptoms was proved to be strictly dependent on the presence of PrP^{C} [9]. Nevertheless, the physiological PrP^{C} functions remain still under investigation, although PrP^{C} has been involved in several cellular processes such as oxidative stress protection [10], copper transport and metabolism [11], membrane excitability and synaptic transmission [12–15], cellular signalling [16,17], neuritogenesis [18], apoptosis [19,20], and neuroprotection [21]. Thus, in this complex scenario, several efforts have been made in order to look for new PrP^{C} binding proteins that could provide new insights into its physiological and pathological functions. Numerous PrP^{C} binding partners located in different cellular compartments were identified, some of which were compatible to sustain the above-hypothesized PrP^{C} functions (reviewed in [22,4]).

In this work, we employed a two-hybrid approach to investigate new potential cellular prion protein interacting partners using a brain expression library. A novel PrP^{C} interacting protein, TREK-1 (TWIK-1-related K^{+} channel) [23], was identified. To our knowledge, TREK-1 is the first membrane channel protein that interacts with PrP^{C}.

Materials and methods

Bacterial two-hybrid assay. The Bacteriomatch® II two-hybrid system (Stratagene, La Jolla, CA, USA) was used to detect protein–protein interactions. A portion of the *Prnp* coding sequence (from 24 to 231 amino acids) was amplified from a rat cerebellum pTRG plasmid cDNA library (Stratagene), using the primers PRNPRn2-U and PRNPRn2-L (Table 1). PCR was performed using 500 ng of plasmid cDNA and with the following thermal profile: 30 cycles at 94 °C × 15 s, 60 °C × 30 s, and 72 °C × 45 s. PCR product was sequenced and *Eco*RI/*Bam*HI subcloned into the pBT *Eco*RI/*Bam*HI linearized vector, thus originating the pBT-PrP recombinant plasmid. According to the manufacturer's instructions, co-transformation of pBT-PrP and pTRG cDNA libraries (200 ng each) was performed using Bacteriomatch® II Screening Reporter Competent cells (Stratagene). Positive control co-transformation experiments were done using the pBT-LGF2 bait and the pTRG-Gal11 target vectors (50 ng each). The screening of the colonies was performed onto Stratagene Dual Selective Screening Medium [5 mM 3-AT (1,2,4-triazol-3-amine), 12.5 μg/ml streptomycin]. Bait (pBT-PrP) and prey plasmids (pTRG) were extracted from each clone (Qiaprep® miniprep kit, Qiagen, Hilden, Germany) and sequenced using the PBTfor and PTRGfor primers (Table 1), respectively. Retransformation of the reporter strain using each purified recombinant pTRG plasmid paired with the pBT-PrP plasmid was performed according to the manufacturer's instructions. Finally, the nucleotide sequences of the target pTRG DNAs were compared to the nucleotide and protein sequence databases using BLAST [24].

Plasmid constructs. For co-immunoprecipitation experiments, pCMV-HA and pCMV-Myc plasmids (Clontech, Palo Alto, CA, USA) were used. A portion of the human *PRNP* coding sequences (23–230 amino acid residues) was amplified from human DNA using the primers PrP23a-U and PrP230a-L (Table 1), *Eco*RI/*Not*I-cloned into the pCMV-HA and pCMV-Myc plasmids, thus originating the pHA/PrP(23–230) and pMyc/PrP(23–230) constructs. Different PrP^{C} deletion constructs were generated into the pCMV-Myc plasmid, specifically pMyc/PrP(23–106), pMyc/PrP(107–230), and pMyc/PrP(128–230); these constructs were produced using the primer pairs PrP23b-U and PrP106-L, PrP107-U and PrP230b-L, and PrP128-U and PrP230b-L, containing *Xho*I and *Not*I restriction sites (Table 1). The entire human *TREK-1* coding sequence, the loop (66–128 amino acid residues), and the carboxyl-terminal (294–411) regions were amplified from 500 ng of human adult brain cDNA (Clontech) with the primer pairs TREK-U and TREK-L, TREK/loop-U and TREK/loop-L, and TREK/Cter-U and TREK-L, respectively. PCR thermal profile was: 30 cycles at 94 °C × 15 s, 62 °C × 30 s, and 72 °C × 60 s. PCR fragments were *Xho*I/*Not*I-cloned into the pCMV-HA and/or pCMV-Myc plasmids.

For the construction of fusion proteins with fluorescent tags, commercial pEGFP-N1 and pDsRed-Express-N1 (Clontech) vectors were used. For the pEGFP-N1/TREK-1 construct, the *TREK-1* coding region was amplified from human brain cDNA using the primers TREK/egfp-U and TREK/egfp-L, and *Xho*I/*Hind*III-cloned into the pEGFP-N1 plasmid upstream the *EGFP* gene. For the construct $pDsRed^{mut}/PrP^{C}$, first, the *RFP* gene was amplified with the primers RFP-U and RFPmut-L, and was cloned into the pDsRed-Express-N1 plasmid *Eco*RI/*Not*I-digested, obtaining the $pDsRed^{mut}$ vector; the PrP^{C} N-terminal signal peptide (1–23) was then amplified from human DNA using the primers PrP1/rfp-U and PrP23/rfp-L and was cloned via *Xho*I/*Eco*RI digestion into the $pDsRed^{mut}$ vector; finally, PrP^{C}(24–252) was amplified with the primers PrP24/rfp-U and PrP252/rfp-L, and was cloned via *Not*I into the $pDsRed^{mut}$ vector.

Cell cultures and transfections. HeLa cells (ECACC, Salisbury, UK) were used for co-immunoprecipitation assays and co-localization experiments. Cells were maintained at 37 °C, 5% CO_2, in DMEM supplied with 10% fetal bovine serum, L-glutamine (1%), 100 U/ml penicillin, and 0.1 mg/ml streptomycin. Cell culture media and supplements were provided by Invitrogen (Carlsbad, CA, USA). Cell transfections were performed with Lipofectamine™ 2000 reagent (Invitrogen) following the manufacturer's instructions.

Western blot analysis and co-immunoprecipitation assays. For immunoblot analysis of HeLa cell extracts, 30 μg of total protein lysate boiled for 5 min in Laemmli sample buffer (2% SDS (w/v), 6% glycerol (v/v), 150 mM β-mercaptoethanol, 0.2% bromophenol blue (w/v), and 62.5 mM Tris–HCl, pH 6.8) and electrophoresed by SDS–PAGE (12% gel). Proteins were transferred onto a nitro-cellulose membrane Hybond™-C Extra (Amersham Biosciences, Little Chalfont, Buckinghamshire, UK). Membranes were blocked with 2% non-fat milk in PBS (phosphate-buffered saline) containing 0.1% Tween™ 20. The following antibodies were employed for immunodetection: monoclonal anti-c-Myc (Clontech), goat polyclonal anti-TREK-1 (TREK-1 C-20, Santa Cruz Biotechnology, Santa Cruz, CA, USA), monoclonal anti-PrP^{C} 3F4 (Sigma, St. Louis, MO, USA), and monoclonal anti-GFP (Roche, Basel, Switzerland), all used at 1:10,000 dilution. Blots were treated with specific peroxidase-coupled secondary antibodies (1:10,000 dilution) and protein signals were revealed by the "ECL Advance™ Western Blotting Detection Kit" (Amersham Biosciences).

Co-immunoprecipitation experiments were performed with total protein extracts derived from HeLa cells transiently over-expressing HA- and Myc-fusion constructs. Total protein extracts were obtained by rinsing the cells twice with ice-cold PBS followed by the addition of ice-cold lysis buffer (1% Triton® X-100, 100 mM NaCl, and 50 mM Tris–HCl, pH 8.0) and by incubating for 30 min in ice. Cell debris were removed by centrifugation at 13,000 rpm for 12 min and supernatant was recovered, quantified by Bradford assay, and supplemented with Complete Mini protease inhibitor cocktail (Roche). Hundred micrograms of total proteins was incubated with 4 μg of the anti-HA antibody for 15 h at 4 °C with gentle agitation. Forty microliters of packed pre-washed protein A sepharose beads (nProtein A 4FastFlow™, Amersham Biosciences) was added to each protein extract and incubated for 1 h 30 min with gentle agitation.

Table 1
Oligonucleotides used in this work

Primer code	5′–3′ Sequence	Restriction site
Bacterial two-hybrid		
PRNPRn2-U	**CCGGAATTC**CGGAAGCGGCCAAAGCCTGGAG	*Eco*RI
PRNPRn2-L	**CGCGGATCC**GCGAGATCTTCTCCCGTCGTAATAGG	*Bam*HI
PBTfor	TCCGTTGTGGGGAAAGTTATC	—
PTRGfor	TGGCTGAACTGGAAGCT	—
Co-immunoprecipitation assay		
PrP23a-U	**GGA ATT CCC** AAG AAG CGC CCG AAG CCT	*Eco*RI
PrP230a-L	**ATT TGC GGC CGC** CGA TCC TCT CTG GTA ATA GG	*Not*I
PrP23b-U	**CCG CTC GAG CG**A AGA AGC GCC CGA AGC CT	*Xho*I
PrP106-L	**ATT TGC GGC CGC** TTT TGG CTT ACT CGG CTT GTT C	*Not*I
PrP107-U	**CCG CTC GAG CG**A CCA ACA TGA AGC ACA TGG CT	*Xho*I
PrP128-U	**CCG CTC GAG CGT** ACG TGC TGG GAA GTG CC	*Xho*I
PrP230b-L	**ATT TGC GGC CGC TTT** CGA TCC TCT CTG GTA ATA GG	*Not*I
TREK-U	**CCG CTC GAG CG**A TGG CGG CCC CTG ACT T	*Xho*I
TREK-L	**ATT TGC GGC CGC TTT A**CT ATT TGA TGT TCT CAA TCA CAG C	*Not*I
TREK/loop-U	**CCG CTC GAG CGT** TGG AGC AGC CTC ATG AGA TT	*Xho*I
TREK/loop-L	**ATT TGC GGC CGC** ATC CCA GTG ACT GAT TTG ATT GG	*Not*I
TREK/Cter-U	**CCG CTC GAG CG**G ATT GGC TCC GAG TGA TAT CT	*Xho*I
Fluorescent proteins		
TREK/egfp-U	**CCG CTC GAG CGG** ATG GCG GCC CCT GAC TT	*Xho*I
TREK/egfp-L	**CCC AAG CTT** TTT GAT GTT CTC AAT CAC AGC AAT C	*Hind*III
PrP1/rfp-U	**CCG CTC GAG** ATG GCG AAC CTT GGC TGC	*Xho*I
PrP23/rfp-L	**CC G AAT TCG** CTT GCA GAG GCC CAG GT	*Eco*RI
PrP24/rfp-U	**ATT T GC GGC CGC T**AA GCG CCC GAA GCC TGG	*Not*I
PrP252/rfp-L	**ATT TGC GGC CGC** TTA TCA TCC CAC TAT CAG GAA GAT GA	*Not*I
RFP-U	**CCG GAA TTC CCA CC**A TGG CCT CCT CC	*Eco*RI
RFPmut-L	**GTC GCG GCC GC**C AGG AAC AGG TGG TGG CG	*Not*I

The bases flanking the gene-specific sequences are in bold; restriction sites (underlined) and endonucleases are indicated.

The beads were washed five times with ice-cold lysis buffer, and the conjugated proteins were eluted by incubation at 95 °C for 5 min in 10 μl of Laemmli sample buffer and subjected to SDS–PAGE and immunoblot analysis.

Co-localization experiments and confocal microscopy analysis. Three micrograms of each construct, pEGFP-N1/TREK-1 and pDsRed^{mut}/PrP^{C}, was transiently transfected in HeLa cells at 95% confluence into 29-mm glass-bottomed dishes. Cells were then incubated for 24 h at 37 °C and 5% CO_2. Images were acquired on a Leica TCS SPII microscopy equipped with the confocal inverted microscopy system Leica DM IRBE, using a 63×, NA 1.32 oil immersion objective. EGFP was excited at 488 nm wavelength with a filtered argon laser; RFP was excited at 557 nm wavelength.

In vivo PrP^{C} and TREK-1 cerebellum co-localization. Sections of rat cerebellum (2-months-old), after fixation by perfusion with saline followed by 4% paraformaldehyde in 0.1 M phosphate buffer, pH 7.3, were cut at the cryostat on the sagittal plane; 12-μm thick sections were obtained and collected on silan-coated slides. The sections were incubated overnight at room temperature with a mixture of primary antibodies, containing mouse monoclonal anti-PrP^{C} (3F4, 1:100, Sigma) and goat polyclonal anti-TREK-1 antibodies (TREK-1 C-20, 1:200, Santa Cruz Biotechnology). After washing, the sections were incubated for 1 h with a mixture of Alexa Fluor® 488-conjugated anti-mouse and Alexa Fluor® 594-conjugated anti-goat secondary antibodies (Invitrogen), both 1:100 diluted. As a negative control staining, sections were incubated omitting the primary antibodies. No immunoreactivity was obtained. After the histochemical procedure, coverslips were finally mounted in a drop of Mowiol® (Calbiochem, Darmstadt, Germany) and observed by fluorescence microscopy with an Olympus BX50 microscope equipped with a 100 W mercury lamp. The following conditions were used: 450–480 nm excitation filter (excf), 500 nm dichroic mirror (dm), and 515 nm barrier filter (bf) for Alexa 488; 540 nm excf, 580 nm dm, and 620 nm bf for Alexa 594. Images were finally recorded with an Olympus Camedia C-2000 Z digital camera.

Results

Bacterial two-hybrid screening and identification of TREK-1 as a protein interacting with PrP^{C}

A coding portion of the rat *Prnp* gene, corresponding to that of the mature PrP^{C} protein, was cloned into the pBT Bacteriomatch® II two-hybrid system bait plasmid and used to isolate putative PrP^{C} interacting proteins in a rat brain cDNA library. Prior to perform the two-hybrid assay, the bait plasmid (pBT-PrP, described in Materials and methods) and the empty vectors, i.e., pBT and pTRG, were individually tested for self-activation of the reporter cassette, in the absence of interacting partners, showing no activation. The pBT-PrP and the pTRG-rat brain cDNA plasmid libraries were then co-transformed into screening reporter competent *Escherichia coli* cells, giving about 10^5 cfu, using a single selective screening medium (5 mM 3-AT, Stratagene). After a more stringent selection on a dual selective medium (5 mM 3-AT and 12.5 μg/ml streptomycin, Stratagene), the number of clones was reduced to 40. This medium was also used to assess the positive control of the system, i.e., the pBT-LGF2 bait and the pTRG-Gal11 prey plasmids, coding for two

interacting proteins. From the above-mentioned 40 clones, the pBT-PrP and the pTRG plasmids were isolated and sequenced. To further confirm the observed interactions, each purified target plasmid along with the recombinant pBT plasmid was co-transformed into the reporter strain, obtaining the growth of the clones onto the dual selective medium. Two pTRG DNA nucleotide sequences were identical and matched to the *Rattus norvegicus* tandem pore domain potassium channel TREK-1 mRNA (AF385402, from nucleotides 432 to 1431). Noticeably, TREK-1 and PrP^C proteins are well conserved in *Homo sapiens* and *R. norvegicus*, showing a 96% and 88% of amino acid identity, respectively.

Verification of PrP^C–TREK-1 interaction using co-immunoprecipitation assay in HeLa cells

To test the interaction between PrP^C and TREK-1, we employed co-immunoprecipitation assays of transiently over-expressed tagged-proteins in HeLa cells. First, we verified the interaction between HA/PrP^C(23–230) and Myc/TREK-1 fusion proteins; thus, PrP^C protein constructs lacking the amino-(from 1 to 22 residues) and carboxyl-(231–252) terminal signal peptides were assayed against the entire TREK-1. As shown in Fig. 1A, Myc/TREK-1 co-precipitates with HA/PrP^C(23–230) constructs confirming the interaction between the two proteins. Moreover, the co-precipitation of the complex was also obtained with the inverted tags, i.e., HA/TREK-1 and Myc/PrP^C(23–230) (Fig. 1B). Mock experiments, performed without anti-HA antibody did not show the immuno-precipitated electrophoretic band.

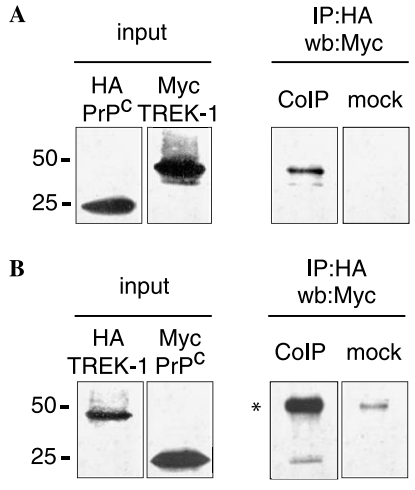

Fig. 1. Co-immunoprecipitation experiments between HA/PrP^C(23–230) and Myc/TREK-1 (A) or HA/TREK-1 and Myc/PrP^C(23–230) (B) fusion proteins. (A) The HA/PrP^C(23–230)-Myc/TREK-1 complex formation, employing anti-HA antibody for immunoprecipitation and anti-c-Myc antibody for detection, was assayed: electrophoretic band corresponding to Myc/TREK-1 construct is about 50 kDa in Co-IP lane, as expected. (B) The interaction between PrP^C(23–230) and TREK-1 was demonstrated with the inverted tags. Asterisk indicates protein A and/or antibody heavy chain; Co-IP, co-immunoprecipitated product; input, protein lysate; IP, immunoprecipitation antibody; mock, negative control; pA, protein A Sepharose; wb, Western blotting antibody.

Characterization of the interaction domains of the proteins employing co-immunoprecipitation assay

To define the domains of interaction alongside the protein sequences, we employed co-immunoprecipitation assays of over-expressed tagged-proteins with deletion constructs for each protein partner. We produced three PrP^C deletion mutants, namely PrP^C(23–106), PrP^C(107–230), and PrP^C(128–230), and tested them individually against the HA-tagged TREK-1 protein. As shown in Fig. 2A, the fusion proteins Myc/PrP^C(107–230) and Myc/PrP^C(128–230) co-precipitated with the HA/TREK-1 construct in the immuno-complex. To further map the TREK-1 interacting region with the PrP^C, two tagged-protein deletions were produced, specifically Myc/TREK-1(66–128) and Myc/TREK-1(294–411). Fig. 2B shows that Myc/TREK-1(294–411) interacted with HA/PrP^C(23–230) fusion protein; differently, Myc/TREK-1(66–128) did not show immuno-precipitated complexes with HA/PrP^C(23–230).

Co-localization experiments of the fluorescent fusion proteins in HeLa cells

In order to investigate if the interaction between PrP^C and TREK-1 could be further sustained by co-localization in living cells, we produced fluorescent fusion proteins of the two interacting candidates. The expression constructs, $pDsRed^{mut}/PrP^C$ and pEGFP-N1/TREK-1, were transiently over-expressed in HeLa cells and visualized using a confocal microscopy. Fig. 3A graphically shows the fusion proteins and the Western blot analysis of the transfected HeLa cells lysates: PrP^C/DsRed fusion protein showed hetero-disperse electrophoretic bands from 50 to 75 kDa; differently, TREK-1/EGFP chimera exhibited two distinct bands of about 77 and 85 kDa. As shown in Fig. 3B, the two proteins shared similar sub-cellular localization signals: fluorescent PrP^C and TREK-1 were both predominantly localized to the plasma membrane, with less intensive co-localization signals within the cell cytoplasm.

Co-localization of the PrP^C and TREK-1 endogenous proteins in the cerebellar cortex

In the cerebellar cortex, the single immunoreaction for PrP^C revealed an intense staining in the molecular layer (ML); in particular, the PrP^C labelled strongly the Purkinje cell somata, the primary dendritic tree, the thin branches, and the spiny branchlets (Fig. 4A). Differently, the internal granular layer (IGL) was very weakly immunostained. After the single immunofluorescence for TREK-1, the Purkinje cell somata were intensely labelled, whereas the dendritic branches were weakly immunoreactive (Fig. 4B). TREK-1 immunoreactivity

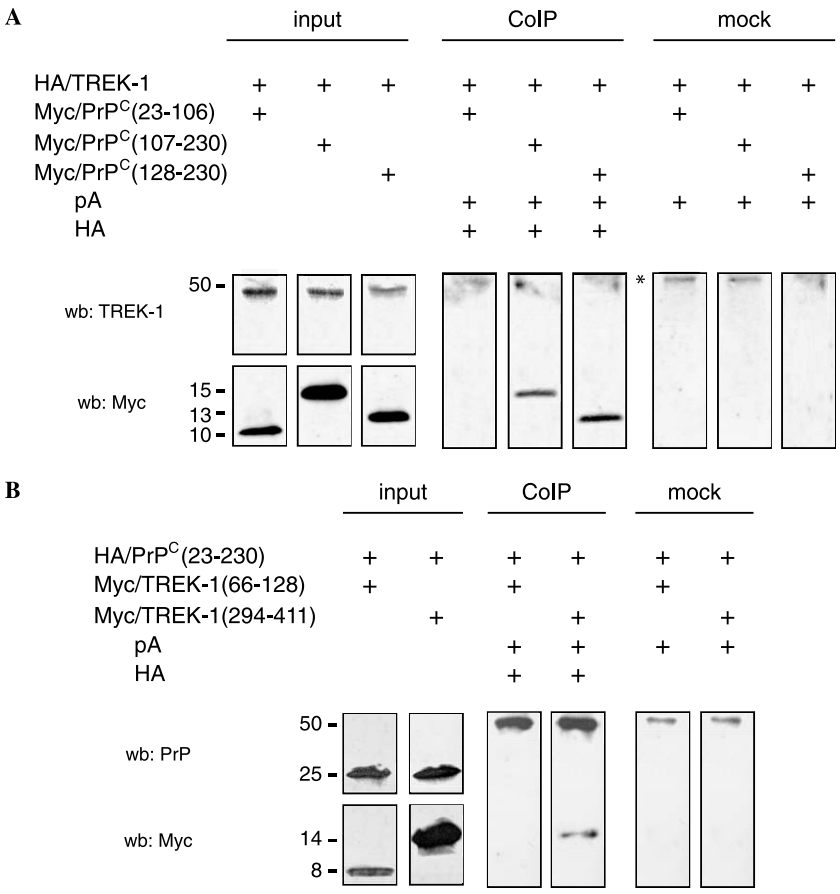

Fig. 2. PrP^C and TREK-1 deletion interaction mapping using co-immunoprecipitation assays. (A) The interaction between TREK-1 protein and the PrP^C carboxyl-terminal domain, specifically Myc/PrP^C(107–230) and Myc/PrP^C(128–230), is shown. No electrophoretic band is detected in the Co-IP lane, in correspondence of the PrP^C amino-terminal domain, Myc/PrP^C(23–106). (B) The panel shows the interaction of the carboxyl-terminal region of TREK-1 protein, i.e., Myc/TREK-1(294–411), versus HA/PrP^C(23–230) fusion protein. Anti-HA antibody for immunoprecipitation was employed; on the left of each Western blotting panel the primary antibodies used are indicated. Asterisk indicates protein A and/or antibody heavy chain.

was faint in the ML and in the IGL. Therefore, the double immunoreaction for PrP^C and TREK-1 showed that the two proteins exhibited co-localization signals in correspondence of the Purkinje cell somata, as shown in Fig. 4C.

Discussion

In this work, we describe a novel interaction between PrP^C and a tandem pore domain potassium channel protein, TREK-1. This interaction was revealed using a bacterial two-hybrid system originally developed by Dove and collaborators [25] and further refined by Joung and collaborators [26]. This system allowed detecting protein–protein interactions in an in vivo *E.coli*-based cell system. While the yeast two-hybrid system has been widely and successfully exploited in protein interaction studies, the bacterial system is likely valuable in reducing the chance that the host harbours an eukaryotic homologue of one of the interacting protein partners that could interfere with important cellular functions.

The investigated cellular prion protein (PrP^C) is a copper-binding glycoprotein [27] predominantly expressed by neurons and glia cells [28,29]. An abnormal isoform of this protein (PrP^{Sc}) is believed to be the primary component of infectivity in prion diseases [30,6]. To date, prion physiological functions are still currently under investigation and several studies have been conducted in the last years in order to investigate novel PrP^C interacting partners. Different protein candidates, such as the laminin and its receptor, p66, N-CAM, GFAP, Bcl-2, and Grb2, were identified, suggesting a role of PrP^C in a multi-functional complex [22,31].

TREK-1 is a recently described two-pore domain potassium channel involved in the background regulation of neuronal membrane excitability: it contains four transmembrane regions and displays both the amino- and carboxyl-terminal domains in the intracytosolic compartment [23,32]. This protein constitutes a mechano-gated channel that is activated by temperature, membrane stretch, and internal acidosis; moreover, it is activated by certain polyunsaturated fatty acids (PUFAs) with neuroprotective activity and by gaseous general anesthetics via a protein kinase A (PKA)-dependent pathway [32,33]. It is of note that, except for PrP^C in this work, no other interactant has been reported so far for TREK-1.

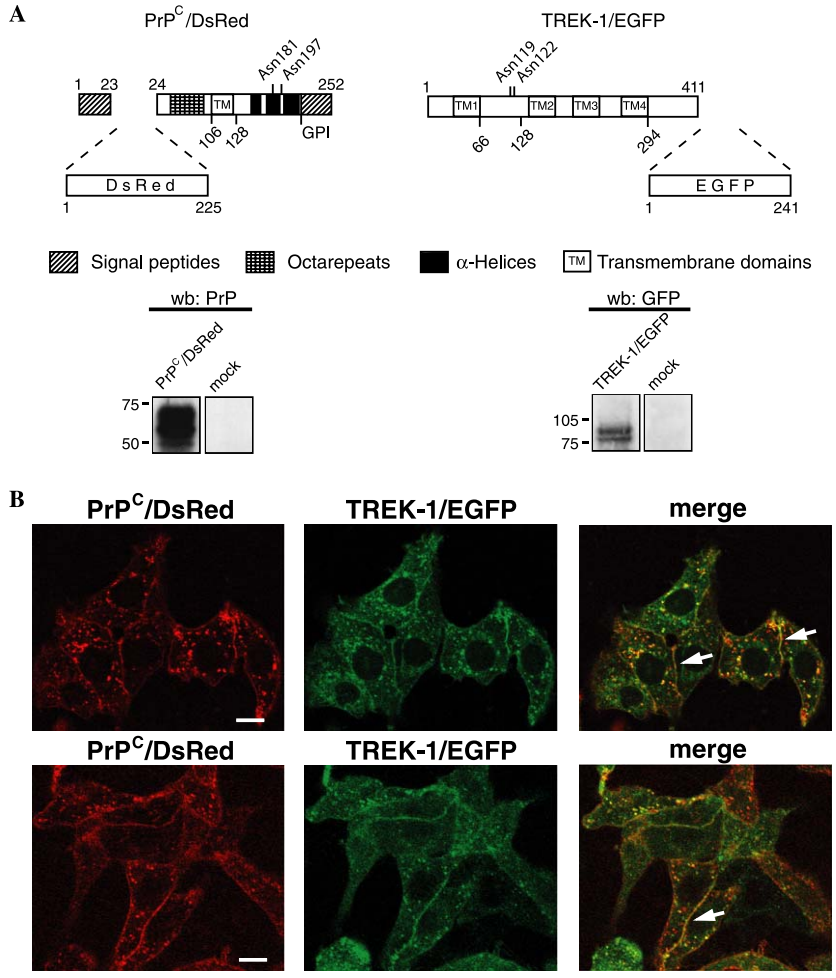

Fig. 3. Chimeric fluorescent proteins used in this work and co-localization experiments. (A) Graphical representations of fluorescent fusion proteins PrP^C/DsRed and TREK-1/EGFP and electrophoretic profiles of the transfected chimera by immunoblot analyses. Biochemical features like signal peptides, α-elices, octarepeats region, transmembrane domain, glycosylation sites, GPI-anchoring site for PrP^C, and transmembrane domains for TREK-1 are indicated. Amino acid coordinates refer to the human protein sequences. Mock controls are non-transfected HeLa cells. (B) PrP^C/DsRed and TREK-1/EGFP fusion proteins transiently expressed in HeLa cells show co-localization signals mostly located to the plasma membranes (arrows) and partially within the cytoplasm. Scale bars: 10 μm.

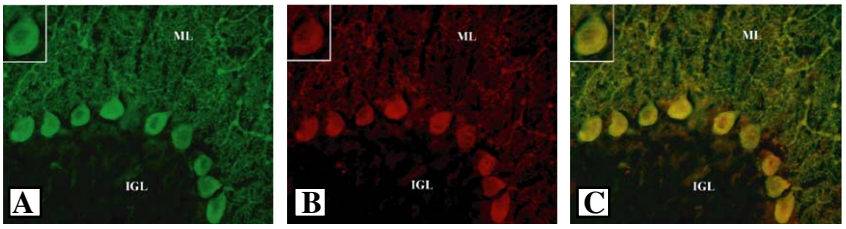

Fig. 4. PrP^C and TREK-1 expression in the rat cerebellar cortex. (A) PrP^C was strongly expressed in Purkinje cell somata (inset), primary dendritic trees, thin branches, and spiny branchlets of Purkinje cells throughout the molecular layer (ML). A weak immunoreactivity was observed in the internal granular layer (IGL). (B) TREK-1 was expressed in Purkinje cell somata (inset) and weakly in the dendritic trees. The TREK-1 labelling was faint within the IGL. (C) Co-localization signals were in correspondence of Purkinje cells somata. Magnifications: 60×.

The results of the PrP^C/TREK-1 interaction, obtained with the two-hybrid assay, were confirmed through co-immunoprecipitation of co-expressed tagged-proteins, HA/PrP(23–230) and Myc/TREK-1, transiently over-expressed in HeLa cells. The complex was further confirmed through the inversion of the bait and prey tagged-proteins. Moreover, an interaction mapping analysis identified the carboxyl-terminal domains of the PrP^C(128–230) and TREK-1(294–411) proteins as the potential interacting regions. In particular, TREK-1 carboxyl-terminal domain has important roles in the physiological function of the channel: this region is crucial for TREK-1 activation by stretch,

temperature, intracellular acidosis, and extracellular lysophospholipids (LPLs) or anesthetics activation [32].

The PrP^C–TREK-1 interaction was also visualized in living eukaryotic cells through a confocal microscopy analysis, employing fluorescent fusion proteins. To exclude interference of the fluorescent protein tags in the physiological post-translational modifications of PrP^C and TREK-1, an immunoblot analysis of the PrP^C/DsRed and TREK-1/EGFP proteins in transfected HeLa cells was performed. In particular, PrP^C/DsRed revealed an hetero-disperse signal of 50–75 kDa, likely attributed to un-, mono-, and di-glycosylated isoforms, similar to the electrophoretic pattern recently described for the GFP-bPrP construct in mammalian transfected cell lines [34]. Furthermore, PrP^C glycoforms heterogeneity has been previously described in cultured cell lines (reviewed in [5] and [35]). TREK-1/EGFP electrophoretic profile showed a pattern composed at least of two bands; these isoforms are likely derived from amino-glycosylation processes, predicted at Asn^{119} and Asn^{122} sites, originating different glycoforms. These sites, located in the loop region of the protein, are similarly conserved in the previously described *R. norvegicus* TREK-2 glycosylated protein, a new member of the two-pore domain potassium channel family [36].

In transiently transfected HeLa cells, we co-localized the fusion proteins to the cellular membrane and, less extensively, in cytoplasmic compartments. To this regard, the precise localization of PrP^C in living cells is largely debated [4]. Whereas some authors reported that PrP^C has predominantly a plasma membrane location, others suggested that PrP^C is present on all biosynthetic and endocytic transport membranous structures and in the cytosol of a subpopulation of neurons in the hippocampus, thalamus, and neocortex [37]. The GPI-anchored outer membrane localization of PrP^C might not completely sustain the interaction with the cytosolic portion of TREK-1. As a matter of fact, the constitutive cycling of the cell surface PrP^C between the plasma membrane and early endosomes [38] could justify our results of the interaction between the carboxyl-termini of the PrP^C and TREK-1 proteins. Furthermore, the interaction between PrP^C and candidate transmembrane proteins to direct PrP^C internalization was recently proposed [39].

To further confirm the in vivo interaction of the two proteins, endogenous PrP^C and TREK-1 were immunolocalized in rat cerebellar cortex sections, mainly in correspondence of the Purkinje cells. In particular, PrP^C immunostained the Purkinje cell layer, similarly to previous results obtained using the same [40] or different anti-PrP^C primary antibodies [41]. The findings of high PrP^C expression in Purkinje cells were also in agreement with mRNA expression studies in rat brain sections [42]. TREK-1 immunostaining was mainly in correspondence of the Purkinje cell layer and, to a lesser extent, within the granular layer, as previously documented [43].

Interestingly, PrP^C has been shown to influence ion transport proteins inducing changes in the lipid bilayer environment and these data suggested a direct effect of PrP^C on ion transport processes [44]. Furthermore, recent in vivo studies revealed that the loss of PrP^C function may interfere with the neuronal intrinsic physiology [45,18], leading to changes in neural networks that might be involved in epileptogenesis [46,47]. Similarly, TREK-1 channels showed peculiar electrophysiological and pharmacological properties [48]. These channels are activated in different conditions following anesthetic treatment, suggesting that it might be a target in the action of anesthetic drug. In addition, TREK-1 plays a major role in the PUFAs/LPLs-induced neuroprotection against epilepsy and ischemia [49–51]. It has been shown that, during the ischemic condition, arachidonic acid is released and TREK-1 channels are activated to protect the cell against excessive and deleterious neuronal excitability and, interestingly, TREK-1 null mice displayed resistance to anesthesia [52].

In conclusion, we have described a novel interaction between the cellular prion protein and the potassium channel TREK-1. To this regard, future works will be directed to investigate the physiological significance of this interaction, in particular if the proteins are involved in common neuroprotective mechanisms.

Acknowledgments

The authors are particularly grateful to Dr. Fiorenzo Peverali for providing eukaryotic expression vectors. This work was supported by a grant from the Ministry for Education, University and Research (MIUR) of Italy "Progetti di Ricerca di Interesse Nazionale" (2005).

References

[1] J.G. Fournier, Nonneural cellular prion protein, Int. Rev. Cytol. 208 (2001) 121–160.
[2] R. Cappai, S.J. Collins, Structural biology of prions, Contrib. Microbiol. 7 (2004) 32–47.
[3] D. Sarnataro, V. Campana, S. Paladino, M. Stornaiuolo, L. Nitsch, C. Zurzolo, PrP(C) association with lipid rafts in the early secretory pathway stabilizes its cellular conformation, Mol. Biol. Cell 15 (2004) 4031–4042.
[4] V. Campana, D. Sarnataro, C. Zurzolo, The highway and byways of prion protein trafficking, Trends Cell Biol. 15 (2005) 102–111.
[5] P.M. Rudd, A.H. Merry, M.R. Wormald, R.A. Dwek, Glycosylation and prion protein, Curr. Opin. Struct. Biol. 12 (2002) 578–586.
[6] S. Prusiner, Prions, Proc. Natl. Acad. Sci. USA 95 (1998) 13363–13383.
[7] K. Basler, B. Oesch, M. Scott, D. Westaway, M. Walchli, D.F. Groth, M.P. McKinley, S.B. Prusiner, C. Weissmann, Scrapie and cellular PrP isoforms are encoded by the same chromosomal gene, Cell 46 (1986) 417–428.
[8] F.L. Heppner, A. Aguzzi, Prion diseases, Encyclopedia of life science (2001) 1–6.
[9] C. Weissmann, E. Flechsig, PrP knock-out and PrP transgenic mice in prion research, Br. Med. Bull. 66 (2003) 43–60.
[10] D.R. Brown, C. Clive, S.J. Haswell, Antioxidant activity related to copper binding of native prion protein, J. Neurochem. 76 (2001) 69–76.
[11] P.C. Pauly, D.A. Harris, Copper stimulates endocytosis of the prion protein, J. Biol. Chem. 273 (1998) 33107–33110.

[12] J. Collinge, M.A. Wittington, K.C. Sidle, C.J. Smith, M.S. Palmer, A.R. Clarke, J.G. Jefferys, Prion protein is necessary for normal synaptic function, Nature 370 (1994) 295–297.
[13] S.B. Colling, J. Collinge, J.G. Jefferys, Hippocampal slices from prion protein null mice: disrupted Ca(2+)-activated K+ currents, Neurosci. Lett. 209 (1996) 49–52.
[14] J.W. Herms, T. Tings, S. Gall, A. Madlung, A. Giese, H. Siebert, P. Schurmann, O. Windl, N. Brose, H. Kretzschmar, Evidence of presinaptic location and function of the prion protein, J. Neurosci. 19 (1999) 8866–8875.
[15] G.R. Mallucci, S. Ratte, E.A. Asante, J. Linehan, I. Gowland, J.G. Jefferys, J. Collinge, Post-natal knockout of prion protein alters hippocampal CA1 properties, but does not result in neurodegeneration, EMBO J. 21 (2002) 202–210.
[16] S. Mouillet-Richard, M. Hermonval, C. Chebassier, J.L. Laplanche, S. Lehmann, J.M. Launay, O. Kellermann, Signal transduction through prion protein, Science 289 (2000) 1925–1928.
[17] L.B. Chiarini, A.R.O. Freitas, S.M. Zanata, R.R. Brentani, V.R. Martins, R. Linden, Cellular prion protein transduces neuroprotective signals, EMBO J. 21 (2002) 3317–3326.
[18] E. Graner, A.F. Mercadante, S.M. Zanata, O.V. Forlenza, A.L. Cabral, S.S. Veiga, M.A. Juliano, R. Roesler, R. Walz, A. Minetti, I. Izquierdo, V.R. Martins, R.R. Brentani, Cellular prion protein binds laminin and mediates neuritogenesis, Brain Res. Mol. Brain Res. 76 (2000) 85–92.
[19] C. Kuwahara, A.M. Takeuchi, T. Nishimura, K. Haraguchi, A. Kubosaki, Y. Matsumoto, K. Saeki, Y. Matsumoto, T. Yokoyama, S. Itohara, T. Onodera, Prions prevent neuronal cell-line death, Nature 400 (1999) 225–226.
[20] L. Solforosi, J.R. Criado, D.B. McGavern, S. Wirz, M. Sanchez-Alavez, S. Sugama, L.A. DeGiorgio, B.T. Volpe, E. Wiseman, G. Abalos, E. Masliah, D. Gilden, M.B. Oldstone, B. Conti, R.A. Williamson, Cross-linking cellular prion protein triggers neuronal apoptosis in vivo, Science 303 (2004) 1514–1516.
[21] X. Roucou, A.C. LeBlanc, Cellular prion protein neuroprotective function: implications in prion diseases, J. Mol. Med. 83 (2005) 3–11.
[22] V.R. Martins, A.F. Mercadante, A.L.B. Cabral, A.R.O. Freitas, R.M. Castro, Insights into the physiological function of cellular prion protein, Braz. J. Med. Biol. Res. 34 (2001) 585–595.
[23] M. Fink, F. Duprat, F. Lesage, R. Reyes, G. Romey, C. Heurteaux, M. Lazdunski, Cloning, functional expression and brain localization of a novel unconventional outward rectifier K+ channel, EMBO J. 15 (1996) 6854–6862.
[24] S.F. Altschul, W. Gish, W. Miller, E.W. Myers, D.J. Lipman, Basic local alignment search tool, J. Mol. Biol. 215 (1990) 403–410.
[25] S.L. Dove, J.K. Joung, A. Hochschild, Activation of prokaryotic transcription through arbitrary protein–protein contacts, Nature 386 (1997) 627–630.
[26] J.K. Joung, E.I. Ramm, C.O. Pabo, A bacterial two-hybrid selection system for studying protein-DNA and protein–protein interactions, Proc. Natl. Acad. Sci. USA 97 (2000) 7382–7387.
[27] D.R. Brown, Metallic prions, Biochem. Soc. Symp. 71 (2004) 193–202.
[28] H.A. Kretzschmar, S.B. Prusiner, L.E. Stowring, S.J. DeArmond, Scrapie prion proteins are synthesized in neurons, Am. J. Pathol. 122 (1986) 1–5.
[29] M. Moser, R.J. Colello, U. Pott, B. Oesch, Developmental expression of the prion protein gene in glial cells, Neuron 14 (1995) 509–517.
[30] A.L. Horwich, J.S. Weissman, Deadly conformations–protein misfolding in prion disease, Cell 89 (1997) 499–510.
[31] V.R. Martins, R. Linden, M.A. Prado, R. Walz, A.C. Sakamoto, I. Izquierdo, R.R. Brentani, Cellular prion protein: on the road for functions, FEBS Lett. 512 (2002) 25–28.
[32] N.P. Franks, E. Honoré, The TREK K_{2P} channels and their role in general anaesthesia and neuroprotection, Trends Pharmacol. Sci. 25 (2004) 601–608.
[33] A.J. Patel, E. Honoré, Properties and modulation of mammalian 2P domain K+ channels, Trends Neurosci. 24 (2001) 339–346.
[34] A. Negro, C. Ballarin, A. Bertoli, M.L. Massimino, M.C. Sorgato, The metabolism and imaging in live cells of the bovine prion protein in its native form or carrying single amino acid substitutions, Mol. Cell. Neurosci. 17 (2001) 521–538.
[35] M. Ermonval, S. Mouillet-Richard, P. Codogno, O. Kellermann, J. Botti, Evolving views in prion glycosylation: functional and pathological implications, Biochimie 85 (2003) 33–45.
[36] H. Bang, Y. Kim, D. Kim, TREK-2, a new member of the mechanosensitive tandem-pore K+ channel family, J. Biol. Chem. 275 (2000) 17412–17419.
[37] A. Mironov Jr., D. Latawiec, H. Wille, E. Bouzamondo-Bernstein, G. Legname, R.A. Williamson, D. Burton, S.J. DeArmond, S.B. Prusiner, P.J. Peters, Cytosolic prion protein in neurons, J. Neurosci. 23 (2003) 7183–7193.
[38] D.A. Harris, Trafficking, turnover and membrane topology of PrP, Br. Med. Bull. 66 (2003) 71–85.
[39] K.S. Lee, R. Linden, M.A. Prado, R.R. Brentani, V.R. Martins, Towards cellular receptors for prions, Rev. Med. Virol. 13 (2003) 399–408.
[40] G.H. Jansen, C.F. Vogelaar, S.M. Elshof, Distribution of cellular prion protein in normal human cerebral cortex–does it have relevance to Creutzfeldt-Jakob disease? Clin. Chem. Lab. Med. 39 (2001) 294–298.
[41] M.M. Esiri, J. Carter, J.W. Ironside, Prion protein immuno-reactivity in brain samples from an unselected autopsy population: findings in 200 consecutive cases, Neuropathol. Appl. Neurobiol. 26 (2000) 273–284.
[42] K. Tanji, K. Saeki, Y. Matsumoto, M. Yakeda, K. Hirasawa, K. Doil, Analysis of PrP^C mRNA by in situ hybridization in brain, placenta, uterus and testis of rats, Intervirol. 38 (1995) 309–315.
[43] C.W. Hervieu, P.J. Green, J.L. Ranson, A.D. Randall, H.J. Meadows, Distribution and expression of TREK-1, a two-pore-domain potassium channel, in the adult rat CNS, Neurosci. 103 (2001) 899–919.
[44] J.I. Kourie, Mechanisms of prion-induced modifications in membrane transport properties: implications for signal transduction and neurotoxicity, Chem. Biol. Interact. 138 (2001) 1–26.
[45] E. Graner, A.F. Mercadante, S.M. Zanata, V.R. Martins, D.G. Jay, R.R. Brentani, Laminin-induced PC-12 cell differentiation is inhibited following laser inactivation of cellular prion protein, FEBS Lett. 482 (2000) 257–260.
[46] R. Walz, O.B. Amaral, I.C. Rockenbach, R. Roesler, I. Izquierdo, E.A. Cavalheiro, V.R. Martins, R.R. Brentani, Increased sensitivity to seizures in mice lacking cellular prion protein, Epilepsia 40 (1999) 1679–1782.
[47] R. Walz, R.M. Castro, T.R. Velasco, C.G. Carlotti Jr., A.C. Sakamoto, R.R. Brentani, V.R. Martins, Cellular prion protein: implications in seizures and epilepsy, Cell. Mol. Neurobiol. 22 (2002) 249–257.
[48] F. Lesage, Pharmacology of neuronal background potassium channels, Neuropharmacol. 44 (2003) 1–7.
[49] A.J. Patel, E. Honoré, F. Maingret, F. Lesage, M. Fink, F. Duprat, M. Lazdunski, A mammalian two pore domain mechano-gated S-like K+ channel, EMBO J. 17 (1998) 4283–4290.
[50] A.J. Patel, E. Honoré, F. Lesage, M. Fink, G. Romey, M. Lazdunski, Inhalation anesthetics activate two-pore-domain background K+ channels, Nat. Neurosci. 2 (1999) 422–426.
[51] F. Maingret, A.J. Patel, F. Lesage, M. Lazdunski, E. Honore, Lysophospholipids open the two-pore domain mechano-gated K(+) channels TREK-1 and TRAAK, J. Biol. Chem. 275 (2000) 10128–10133.
[52] C. Heurteaux, N. Guy, C. Laigle, N. Blondeau, F. Duprat, M. Mazzuca, L. Lang-Lazdunski, C. Widmann, M. Zanzouri, G. Romey, M. Lazdunski, TREK-1, a K+ channel involved in neuroprotection and general anesthesia, EMBO J. 23 (2004) 2684–2695.